

# Influence of Motion Restrictions in an Ankle Exoskeleton on Gait Kinematics and Stability in Straight Walking

Miha Dežman, Charlotte Marquardt, Adnan Üğür and Tamim Asfour

**Abstract**—Exoskeleton devices impose kinematic constraints on a user’s motion and affect their stability due to added mass but also due to the simplified mechanical design. This paper investigates how these constraints resulting from simplified mechanical designs impact the gait kinematics and stability of users by wearing an ankle exoskeleton with changeable degree of freedom (DoF). The exoskeleton used in this paper allows one, two, or three DoF at the ankle, simulating different levels of mechanical complexity.

This effect was evaluated in a pilot study consisting of six participants walking on a straight path. The results show that increasing the exoskeleton DoF results in an improvement of several metrics, including kinematics and gait parameters. The transition from 1 DoF to 2 DoF is shown to have a larger effect than the transition from 2 DoF to 3 DoF for an ankle exoskeleton. However, an exoskeleton with 3 DoF at the ankle featured the best results. Increasing the number of DoF resulted in stability values closer the values when walking without the exoskeleton, despite the added weight of the exoskeleton.

## I. INTRODUCTION

The ankle joint has three degrees of freedom (DoF) and can support loads up to four times the weight of the human body [1]. It also plays a crucial role in generating positive power while walking [2]. Exoskeleton devices that assist the ankle joint demonstrated significant decreases in metabolic energy expenditure [3] during support of straight walking, where ankle plantar-/dorsiflexion (PF/DF) movement is the most notable and the primary focus of the specific exoskeleton design. However, exoskeleton designs should allow for all three rotations of the ankle, as the ankle undergoes movement in all three degrees of freedom (DoF) even during straight walking [4]. Furthermore, the ankle in-/eversion (IN/EV) and internal/external rotation (IR/ER) DoF are also more prominent when turning and walking on curved paths [5]. As a result, exoskeletons designed to solely support straight walking lack the versatility required for daily activities.

The kinematic compatibility, i. e., ability to adapt to the posture of a human joint, depends on the adaptability and DoF of a specific design of the exoskeletons’ frame and kinematics, as explored in our previous work [5]. The exoskeleton frame serves as the mechanical structure responsible for holding the exoskeleton components in place and transmitting the actuation torque to the cuffs. Designing ankle exoskeletons with 3 DoF involves a trade-off, and may quickly lead to increased mechanical complexity and weight

in rigid designs, or a decrease in actuation forces in softsuit designs, as analysed in [5].

The number of DoFs of an ankle exoskeleton affects the motion and stability of the user, however, few studies have directly assessed this effect. Choi et al. [6] showed that a 2 DoF powered ankle-foot orthosis (PAFO) improved the user’s stability significantly compared to a 1 DoF PAFO. Using ski boots, Olivier et al. [7] investigated the effects of ankle restriction on hip and knee kinematics. The results showed more changes in hip kinematics compared to the knee joint. Moreover, they observed that individuals adjust to the imposed restrictions with different strategies. McCain et al. [8] investigated the effect of restrictions on the ankle, knee and hip when using a 3D printed ankle stay and a knee brace to systematically limit the motion of these joints. Restrictions revealed a detrimental effect on the metabolic expenditure of walking, reducing the peak ankle power and knee range of motion (RoM). According to Ranaweera et al. [9], restricting non-sagittal motions also affects muscle activation and causes significant changes in muscle activities. These studies show that restrictions of DoFs has a large effect on kinematics and stability.

The literature put more emphasis on analyzing the influence of weight and inertia on gait, energetics and kinematics. Heavy exoskeletons affect the RoM of the ankle and knee and decrease the foot acceleration in the anteroposterior (AP) direction [10]. Added inertia with 3.5 kg increases the swing times and affects anterior-posterior motion of both the pelvis and the head-arm-trunk segment [10]. Longer and slower strides are also observed by [11]. In addition, Jin et al. [12] also reports reduction in step height and maximum knee flexion. The placement of the supplementary weight is crucial, with distally placed weights intensifying the metabolic rates needed for leg swing, as reported by [11]. Longer strides reduce the AP margin of stability, which is the ability to keep moving forward [13]. The negative influences of supplementary weight and inertia are intertwined with the negative effects of the kinematic restrictions. Therefore, a thorough analysis should take into account both aspects.

The exoskeleton design requires a balance between mechanical complexity, strength and device weight. A lighter yet strong enough exoskeleton design may reduce the weight burden, however, it may also introduce limitations on kinematics and stability. In this paper, we investigate the effects of the number of DoF in an ankle exoskeleton on the user’s gait, ankle kinematics and stability. The participants walked with an exoskeleton that could simulate a one, two, or three DoF at the ankle, thereby representing different levels of

This work has been supported by the Carl Zeiss Foundation through the JuBot project.

The authors are with the High Performance Humanoid Technologies Lab, Institute for Anthropomatics and Robotics, Karlsruhe Institute of Technology (KIT), Germany. {miha.dezman, asfour}@kit.edu

mechanical complexity. We measured various gait parameters such as stride length, time, and height, as well as cuff rotation and the RoM. Specifically, we analyzed the average values for PF/DF, IN/EV and IR/ER, their RoM and similarity. Furthermore, our study investigates how these limitations affect the user’s stability.

The rest of the paper is organized as follows. Section II describes the exoskeleton, user study, data postprocessing and analysis methods. Section III reports and analyzes the results of the user study. Section IV discusses the implications, limitations, and future work of this paper. Section V concludes the paper.

## II. MATERIALS AND METHODS

This section introduces the design of the exoskeleton and the motion restriction method. It describes the conducted user study as well as the gait kinematic and stability metrics used to analyze the collected motion capture data.

### A. Exoskeleton and DoF restriction

The ankle exoskeleton used in the study has been previously presented in [5]. It features a rigid frame design composed of a shank and foot section, shown in Fig. 1 (left). Both sections are joined through a parallelogram mechanism and multiple joints enabling all three rotations of the ankle, as shown in Fig. 1 (right). An additional foot frame DoF

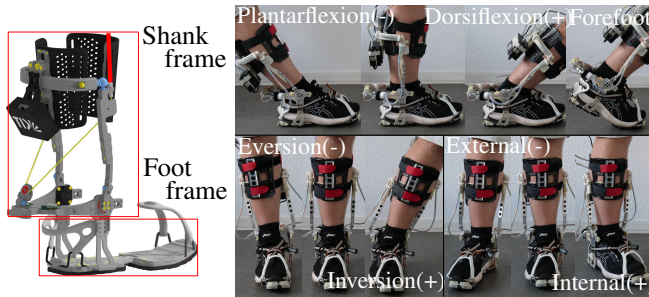


Fig. 1: **Left:** Shank and foot sections of the exoskeleton. **Right:** The exoskeleton during the three rotations: plantar-/dorsiflexion (PF/DF), in-/eversion (IN/EV), and internal/external rotation (IR/ER) of the ankle joint, as well as the forefoot rotation of the foot frame. (adapted from [5])

allows for forefoot rotation.

Figure 2 shows the relevant kinematic joints for the 3 DoF motion and size adjustment as well as the resulting three configurations of the exoskeleton *Exo3DoF*, *Exo2DoF*, and *Exo1DoF*. The foot frame is adjustable in several dimensions, as denoted by adjustable translation joints in Fig. 2. This includes adjustment of length and width to accommodate different sizes and types of shoes.

To restrict the human ankle DoF different exoskeleton frame joints must be immobilized. By mounting fixture elements, i.e., blocking parts, on the existing exoskeleton structure, the ankle joint’s DoF can be reduced from three to either two or one resulting in the three configurations *Exo3DoF*, *Exo2DoF*, and *Exo1DoF*. The following describes how the design restrictions were implemented.

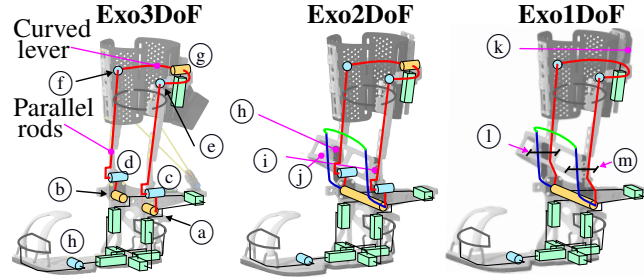


Fig. 2: The three exoskeleton configurations: *Exo3DoF*, *Exo2DoF*, and *Exo1DoF*. The kinematic structure comprises various joint types: a hinge joint represented by “”, a ball joint “”, a hinge joint with angle measurement “”, and an adjustable translation joint “”. The explanations for each callout are provided in the text. (adapted from [5])

The unrestricted 3 DoF kinematics, i.e., the *Exo3DoF* case is shown in Figure 2 (left). It features three hinge joints with integrated angle measurement marked with (a), (b) and (g), where (a) and (b) enable PF/DF. The IN/EV is enabled by hinge joints (c), (d) and (g), which are orthogonal to the parallel rods and the axis of hinge joints (a) and (b). Additionally, the IR/ER is enabled by ball joints (e) and (f).

In the *Exo2DoF* case, the exoskeleton mechanism restricts the IR/ER by adding parts (i), (j) and (h). These constrain the rotation of hinge joints (a) and (b). Consequently, the exoskeleton allows for PF/DF and IN/EV of the ankle.

In the *Exo1DoF* case, the IN/EV is restricted by screwing parts (i) and (j) to the parallel rods, as denoted by (l) and (m). Furthermore, a fourth fixture part is added to constrain the hinge joint (g). Consequently, only PF/DF motion is possible.

The *ExoXDoF* configurations of DoF restrictions, i.e., *Exo1DoF*, *Exo2DoF* or *Exo3DoF*, are chosen according to the most commonly reported DoF combinations in ankle exoskeletons [14]. The entire ankle exoskeleton weighs 1.8 kg, wherein the foot frame section weighs 0.65 kg. The fixture elements together weigh 100 g. The exoskeleton is used passively; however, it has been designed to facilitate cable-driven actuation for plantar flexion motion in the future.

### B. User Study

The goal of the user study is to assess how the exoskeleton DoF constraints influence the kinematics, stability, and gait parameters of individuals while wearing the exoskeleton and walking straight. Six healthy participants (four males and two females) took part in the study. Their information is summarized in Table I. All participants provided written informed consent before the study participation and all methods were performed in accordance with the Declaration of Helsinki. The experiment protocol was approved by the

TABLE I: Participant Information

Height [cm]	Weight [kg]	EU shoe size	Age [y]
177.7 ± 9.3	77.7 ± 24.9	42.7 ± 2.5	24.5 ± 2.6

Values represent the mean and standard deviation.

Karlsruhe Institute of Technology (KIT) Ethics Committee under ethical application for the JuBot project.

Each participant walked with a self-selected speed along a 3 m straight path, turned around, walked back, and returned to the initial pose. The walking path length was maximized while ensuring full motion capture functionality. Each participant study session started with four repetitions of the *NoExo* condition to establish a baseline measurement without the exoskeleton. The three exoskeleton configurations followed, namely: *Exo1DoF*, *Exo2DoF* and *Exo3DoF*, in a randomized order. Same as for the *NoExo* condition, each of the three configurations was repeated four times. Each participant had a 3 min long familiarization phase before the session and resting pauses between conditions and repetitions.

The *NoExo* case was performed without wearing of the exoskeleton and serves as a baseline. In the configurations *ExoXDoF*, the participants wore the exoskeleton on their right leg (1.8 kg), where the exoskeleton allowed the  $X$  number of DoF. The DoF restriction approach was already explained in Fig. 2. The users also wore a foot frame on their left leg (0.65 kg), to account for the thickness of the exoskeleton sole.

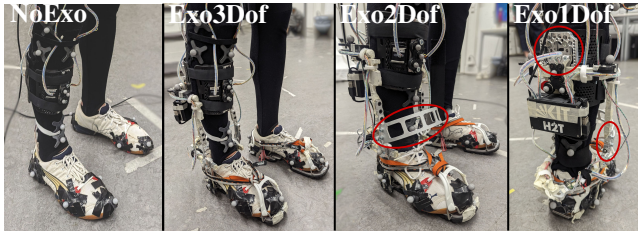


Fig. 3: A participant without and with the ankle exoskeleton in its three configurations. The parts added to fix certain DoF are marked in red.

The exoskeleton was adjusted during the donning process according to the visual inspection and the user's verbal comments regarding comfort and alignment. A well-aligned exoskeleton features minimum vertical sliding of the shank cuff during PF/DF. The motion of both the exoskeleton and the participant in the study was recorded by an optical Motion Capture (MOCAP) system (Vicon Motion System, Ltd, UK). Passive markers were attached to the exoskeleton and participant in a way that ensured a continuous tracking of the markers needed to calculate all three rotations of the ankle joint in all configurations. The marker configuration on the human body is shown in Fig. 3 and Fig. 4. In addition to the MOCAP data, the exoskeleton sensor data was also collected, including force myography (FMG) measurements, which are used in a different study that assesses the change of FMG signals due to the different restrictions in the exoskeleton conditions.

### C. Stride Segmentation

All parameters and signals were evaluated on a stride basis, therefore all raw measurements were segmented into strides and averaged. The angles were segmented using the

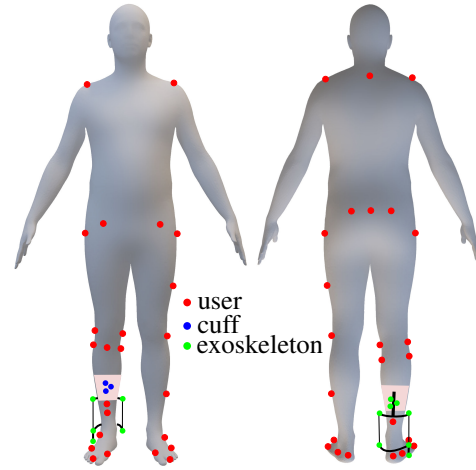


Fig. 4: MOCAP marker positions on the exoskeleton and the user. Red markers are attached on the user. Blue markers are attached on the exoskeleton cuff. Green markers are attached on the exoskeleton.

heel switch activation as seen in Fig. 5 (top left). All transient steps were removed to avoid starting and ending transitions. The selection criterion was the crossing of the zero absolute position of the  $X$  axis, as seen in Fig. 5 (bottom).

### D. Gait Parameters

The analyzed gait parameters used to assess the effect the DoF reduction has on participant gait include:

- 1) *stride length*, analyzed for both legs, denoting the distance from one heel strike to the next heel strike (shown in Fig. 5 (top right)). The stride length is analysed for each leg independently.
- 2) *stride width* denotes the maximum distance between both legs (shown in Fig. 5 (top right)).
- 3) *stride time* denotes the time between two heel strikes.
- 4) *foot height* denotes the maximum height of the foot during a stride for each leg independently.

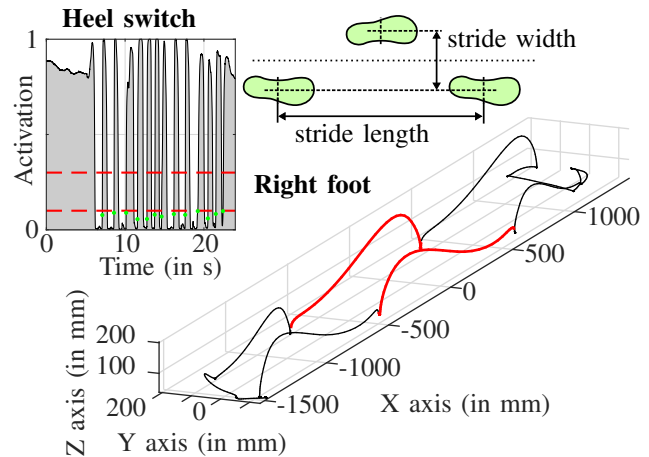


Fig. 5: **Top left:** heel switch activation and detected strides in green. **Bottom:** an example of two segmented strides of the left leg. **Top right:** the stride length and width definition.

### E. Kinematics

The effect on a user's kinematics is determined by observing the three ankle motions: PF/DF, IN/EV, and IR/ER. For each angle, the averages and standard deviations of all strides of all participants were calculated for each exoskeleton configuration. The root-mean-squared error (RMSE) was used to compare the joint angle trajectories of *ExoXDoF* against the *NoExo* condition. A lower RMSE indicates a higher degree of similarity between two conditions. The RoM denotes the maximum and minimum values of the trajectory average and the maximum and minimum standard deviation reached during the gait cycle.

Additionally, the rotation of the shank cuff around the shank axis is measured using markers placed on the exoskeleton and on the user. The shank cuff rotation indicates the angle between the cuff and the knee joint. An increased cuff rotation indicates more movement of the knee relative the shank cuff. This means the presence of IR/ER motion despite the exoskeleton restriction, due to the compliance of the soft tissues around the shank.

### F. Stability

The participant stability is evaluated using a stabilogram of the trunk roll and pitch acceleration, as outlined in [6]. Maintaining balance of the upper body is important to avoid falling. Therefore, the stability is assessed based on the magnitudes of the detected accelerations of the upper body. To quantify them, a Gaussian ellipsoid is fitted onto the accelerations, and its two eigenvalue vectors are used to calculate a root-mean-square (RMS) value representing the instability. According to [6], a higher RMS value, i.e., the instability value, denotes greater swing of the trunk and indicates lower stability of the user. In the current study, trunk accelerations are calculated based on marker motion, positioned in the lower back and between the shoulder girdle. However, an inertial measurement unit (IMU) based system may also be used [6].

## III. RESULTS AND ANALYSIS

### A. Angle and RoM

This section presents angle measurements and RoM results. Figure 6 shows the averages and standard deviations of all strides for the three ankle rotations (PF/DF, IN/EV and IR/ER) and all configurations. The averaged curves

maintained a similar in shape in all configurations compared to the *NoExo* condition. However, some discrepancies were observed. A slight phase delay was observed for PF/DF and IR/ER for all exoskeleton conditions compared to the *NoExo* condition. The standard deviation of *NoExo* condition is generally small but increases at push-off (60%), especially for PF/DF and IN/EV. The exoskeleton configurations feature a similar standard deviation for all strides for IN/EV and IR/ER compared to the *NoExo* condition. However, the standard deviation is higher for PF/DF. The most prominent differences between the shape of all curves are evident in IR/ER. In this case, the *Exo1DoF* curve is flat in the first 0% to 40% of gait cycle. Changing the exoskeleton to the 2 DoF configuration results in an increase in angle magnitudes, but only *Exo3DoF* returns its shape closer to the shape of the *NoExo* curve.

The similarity between curves is better depicted in Fig. 7. For PF/DF, *Exo3DoF* is the most similar to the *NoExo*

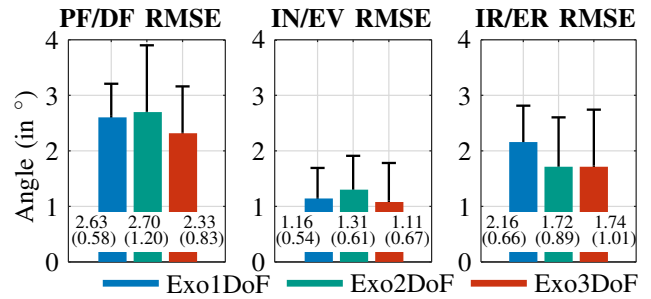


Fig. 7: Ankle rotation similarity of *ExoXDoF* to *NoExo* condition. The RMSE values are calculated between the averages of the respective configuration and the *NoExo* average for all strides of all participants. The standard deviation (vertical error lines) of RMSE values shows variability between the participants.

case, as depicted by the smallest RMSE value. For IN/EV, *Exo3DoF* features the smallest RMSE value, however, the similarity is similar to the *Exo1DoF* case. For IR/ER, the values of *Exo3DoF* and *Exo2DoF* are similar, but lower than *Exo1DoF* case.

Finally, Fig. 8 shows the RoM of the average curves of Fig. 6. The PF/DF RoM shifts with the introduction of the exoskeleton but appears to shift closer to the RoM of the *NoExo* case with the increasing DoF. IN/EV RoM

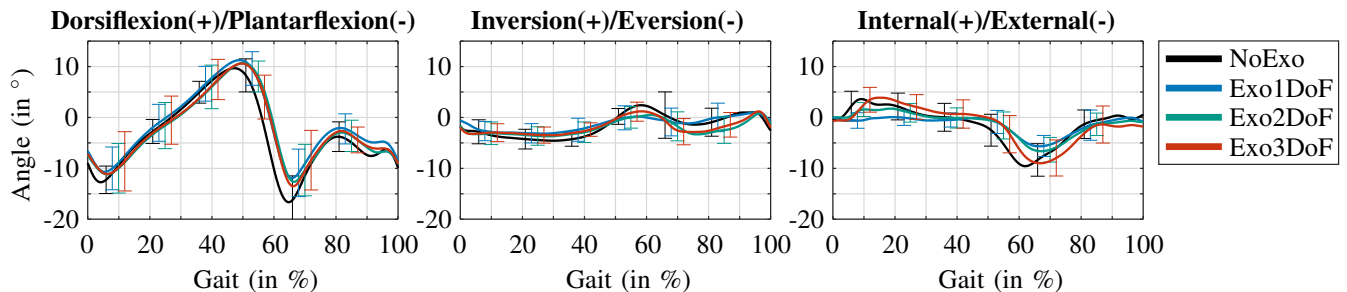


Fig. 6: Average of ankle PF/DF, IN/EV and IR/ER of all strides shown for each configuration. The motion direction is indicated in the title of the subfigures. Error bars indicating the standard deviation of all strides are also given.

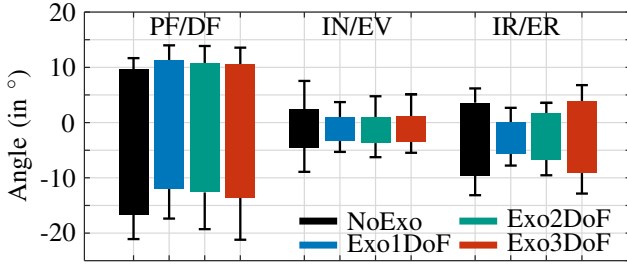


Fig. 8: RoM for all three ankle rotations during straight walking for all configurations (*NoExo*, *Exo1DoF*, *Exo2DoF* and *Exo3DoF*). The blocks represent the maximum and the minimum angle of Fig. 6. The error ticks represent the maximum and minimum when standard deviation is added/subtracted from the curve.

shows only a small improvement with the increase of DoF. IR/ER RoM features the highest improvement of RoM with increasing DoF and returns it to the RoM of the *NoExo* case.

### B. Gait parameters

This section presents the resulting gait parameters: stride time, foot height, stride length, and width. The stride time and foot height are shown in Fig. 9. Wearing of the exoskele-

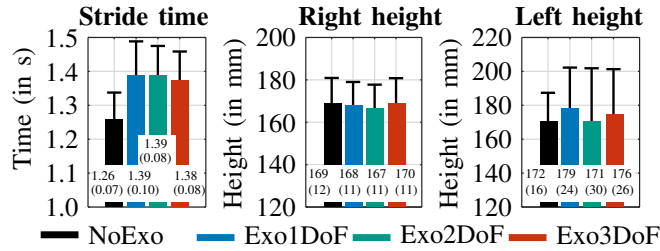


Fig. 9: The left graph displays the average stride duration of all participants for each condition. The middle graph illustrates the maximum height reached by the right foot during a stride, while the right graph shows the same for the left leg. The vertical error lines represent the standard deviation, indicating the variation between participants.

ton increases the stride time with slight time improvement as the number of DoF increases towards the *NoExo* condition. The average and standard deviation of the height of the right foot remain nearly the same throughout all configurations. However, the average and standard deviation of the left foot height fluctuate when changing between configurations.

The stride length for both feet and the stride width for each condition are shown in Fig. 10. The right leg stride length, i. e., the side wearing the exoskeleton, shows decreased step length for all *ExoXDoF* configurations. Changing the number of DoFs did not noticeably affect it. Left stride length decreases for *ExoXDoF* configurations. Both the left and right strides show a comparable standard deviation that does not change during the conditions. The stride width increases with the increase of DoF, in addition, the standard deviation becomes smaller.

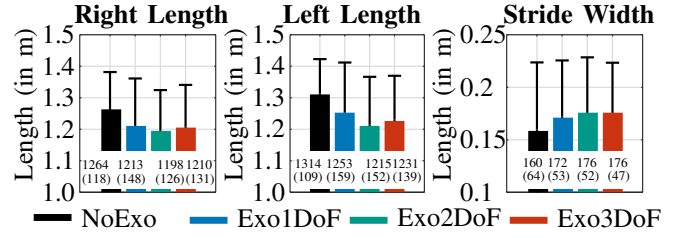


Fig. 10: The left graph shows the average time and standard deviation of all the strides of all participants shown for each condition. The middle and right graphs show the average stride length and standard deviation for the left and right legs, respectively, across various configurations, for all strides of all participants.

The relative cuff rotation displayed in Fig. 11 (left) offers a deeper look on the behaviour of IR/ER between different configurations. The cuff rotation is the largest for the

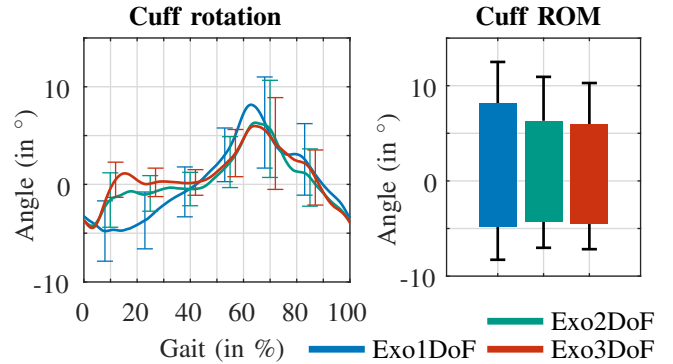


Fig. 11: The left graph shows the average cuff rotation for all strides of all participants shown for each condition. The error bars represent the standard deviation of all strides. The blocks represent the maximum and minimum rotation of the cuff shown in the left graph. The error ticks represent the maximum and minimum when standard deviation is added/subtracted from the curve.

*Exo1DoF* case. With increasing the number of DoF, the relative rotation of the cuff starts to decrease, indicating smaller rotations of the cuff relative to the knee. Condition *Exo3DoF* displays the smallest rotation.

Figure 11 (right) presents the RoM values. Changing from *Exo1DoF* to *Exo2DoF* shows a noticeable decrease in cuff RoM. However, changing from *Exo2DoF* to *Exo3DoF* does not show a noticeable improvement in cuff RoM.

### C. Stability evaluation

Figure 12 (left, middle) displays the average roll and pitch accelerations of the trunk. The *NoExo* condition features the highest accelerations. However, wearing the exoskeleton (*ExoXDoF* condition) reduced some of the acceleration peaks compared to *NoExo* condition. Furthermore, several acceleration peaks of the *NoExo* condition appear to precede those of the *ExoXDoF* condition.

The stabilograms and instability shown in Fig. 13 are based on data from Fig. 12. Figure 13 (left) shows an

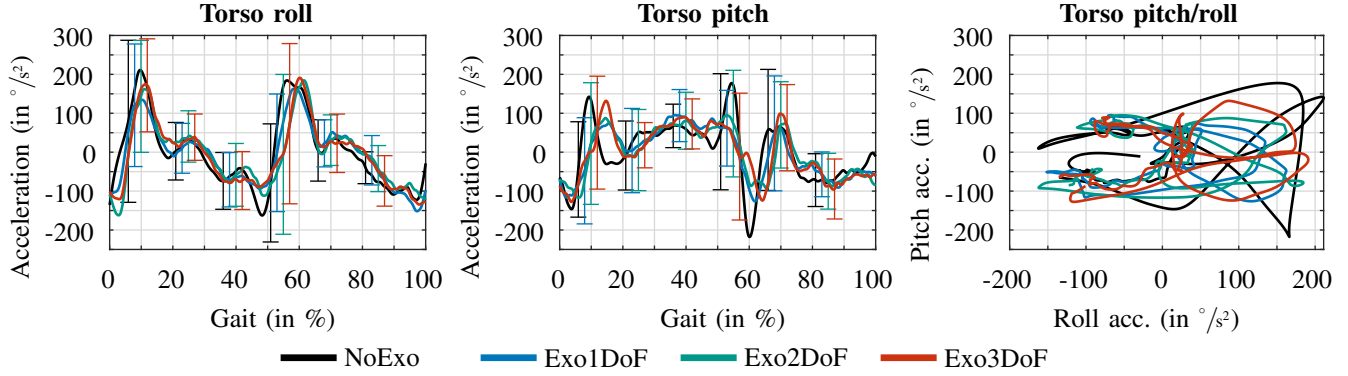


Fig. 12: The left graph shows the average torso roll acceleration for all the strides of all participants shown for all conditions. The error bars represent the standard deviation of all strides. In the same way, the middle graph shows the average acceleration of the torso pitch with the standard deviation. The right graph shows the correlation of both accelerations in a 2D representation.

example Gaussian ellipsoid fit ( $1\sigma$  and  $2\sigma$ ) for the Pitch/Roll accelerations for the *Exo3DoF* case with the corresponding eigenvectors. Figure 13 (middle) shows the ellipsoids ( $1\sigma$ ) and the eigenvectors for all configurations. Figure 13 (right) shows the resulting instability based on the RMS of the corresponding eigenvectors shown for each configuration. Wearing of the exoskeleton (configurations *ExoXDoF*) results in a smaller ellipsoid (see Fig. 13 (middle)) and consequently lower instability values. The ellipsoid becomes larger, especially wider in roll axis, by releasing the DoF restriction from 1 DoF to either 2 DoF or 3 DoF. The change from 1 DoF to 2 DoF is greater than the one from 2 DoF to 3 DoF. Figure 13 (right) shows the highest variability (standard deviation) between participants for the *NoExo* case. However, wearing the exoskeleton (*ExoXDoF*) reduces the standard deviation, indicating that it introduces some restrictions that are similar between participants. Removing the exoskeleton restrictions DoF, i. e., moving to the configuration *Exo3DoF*, enhance instability values but does not restore them to the

*NoExo* values.

#### IV. DISCUSSION

The study shows that wearing the exoskeleton results in a noticeable impact on the user's kinematics, gait parameters and stability. Increasing the number of DoF improved the kinematic compatibility of the exoskeleton, demonstrated by a larger RoM of PF/DF and IR/ER. However, IN/EV does not show the same level of improvement. Increased DoF improves stride time, reduces cuff rotation relative to the knee, and increases the instability value. However, the instability values in [6] demonstrated a different effect showing a decrease when switching from the 1 DoF to 2 DoF configuration. Our study demonstrated the opposite behavior, as the instability value increased with more DoF, resulting in reduced stability of the participant. Based on our findings, the exoskeleton device discussed in [6] induces greater restrictions on users while wearing the 2 DoF exoskeleton in an unpowered case. While [6] does not provide stability

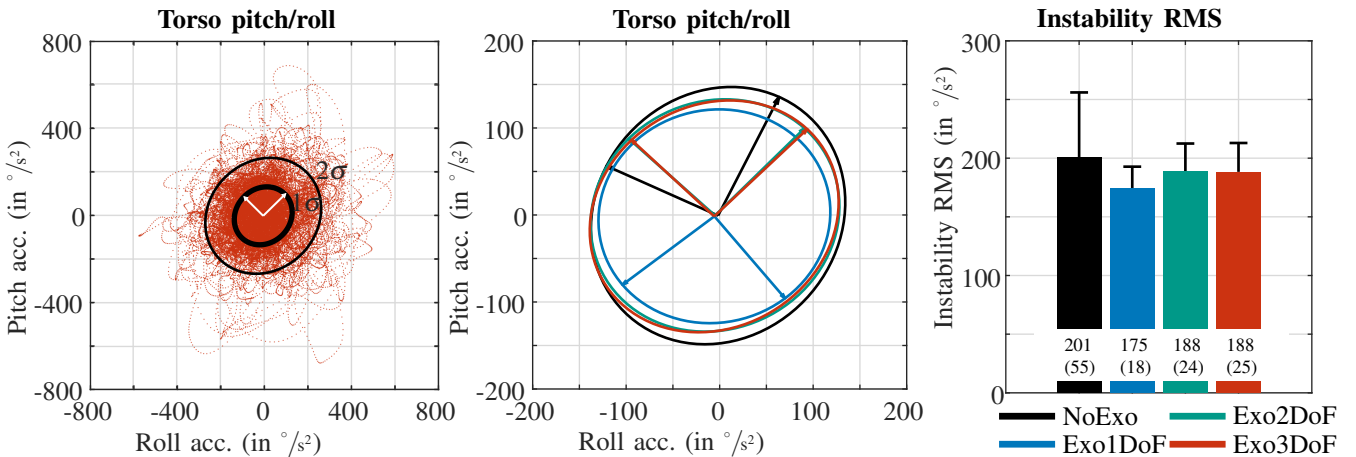


Fig. 13: The left graph shows the torso acceleration data for roll and pitch rotation and the corresponding Gaussian ellipsoid fit for the *Exo3DoF* configuration. The middle graph displays the Gaussian ellipsoids for all configurations. The right graph presents the mean instability value for each configuration, averaged over all participants. The error bars indicate the standard deviation for the averages of all participants.

values without the exoskeleton, additional investigation is required to validate these findings.

The criteria related to IR/ER, that is RMSE value from Fig. 7, cuff rotation values from Fig. 11, and the stability values in Fig. 13 (right), revealed larger improvements when transitioning from 1 DoF to 2 DoF than when transitioning from 2 DoF to 3 DoF. In contrast, restriction of the exoskeleton IR/ER has a limited influence on the IR/ER rotation of the ankle, since rotation is still possible due to the soft tissues around the shank. This is shown in Fig. 11 (right), as even under DoF restrictions the ankle can move, especially in IR/ER. It is expected that the IR/ER becomes more relevant when an ankle exoskeleton is combined with a knee exoskeleton.

This work has limitations related to both the exoskeleton and study design and execution. The exoskeleton's weight (1.8 kg) is the first hardware limitation, negatively affecting the gait. Previous studies have shown that adding weight loads on the foot increases stride length and time, and decreases step height [11], [12]. Our study demonstrated longer stride times while wearing the exoskeleton and a shorter stride length. However, foot height remained similar between conditions. Therefore, the added weight does not have the same influence as reported in previous studies. A possible explanation is that the exoskeleton prompted users to adapt a more cautious walking style, leading to slower and shorter strides. The short walking path also played a role in this, as it prevented the users from achieving a stable gait. A longer path would enable the users to adapt to the exoskeleton and walk more naturally, once they reached a stable gait.

The rigid sole is another hardware limitation that negatively affects the selected criteria. Previous studies have shown that rigid-soled shoes cause short phase delays in the average curves [15]. We observed the same phenomenon in our study, as shown in Fig. 6. Therefore, the removal of the rigid sole is identified as an important next step in the development of this exoskeleton. Moreover, the exoskeleton's adjustments were insufficient for one of the six participants. Therefore, the next exoskeleton iteration will also feature a larger manual adjustment range.

## V. CONCLUSION

This paper addressed the impact of DoF reductions on users and the role of ankle DoF in restoring ankle kinematics, gait parameters, and stability for straight walking. The findings demonstrated that enabling of IN/EV on the exoskeleton yielded greater improvements compared to subsequently adding IR/ER rotation. However, the greatest improvement was observed when the ankle exoskeleton allowed for all three DoF. It is expected that IR/ER becomes more important when the ankle exoskeleton includes a knee joint. This implies that exoskeletons featuring solely PF/DF might benefit from extensions to the other DoF.

For future work, we are developing a second iteration of the ankle exoskeleton with a knee joint extension. The device

will have a lighter frame and a flexible sole. These improvements will enable further investigations of the findings of this study.

## REFERENCES

- [1] R. P. Kleipool and L. Blankevoort, "The relation between geometry and function of the ankle joint complex: A biomechanical review," *Knee Surgery, Sports Traumatology, Arthroscopy*, vol. 18, no. 5, pp. 618–627, May 2010.
- [2] G. S. Sawicki and D. P. Ferris, "Mechanics and energetics of level walking with powered ankle exoskeletons," *Journal of Experimental Biology*, vol. 211, no. 9, pp. 1402–1413, May 2008. [Online]. Available: <https://journals.biologists.com/jeb/article/211/9/1402/18202/Mechanics-and-energetics-of-level-walking-with>
- [3] K. L. Poggensee and S. H. Collins, "How adaptation, training, and customization contribute to benefits from exoskeleton assistance," *Science Robotics*, vol. 6, no. 58, p. eabf1078, Sep. 2021.
- [4] J. D. Hsu, J. W. Michael, J. R. Fisk, and American Academy of Orthopaedic Surgeons, Eds., *AAOS Atlas of Orthoses and Assistive Devices*, 4th ed. Philadelphia: Mosby/Elsevier, 2008.
- [5] M. Dežman, C. Marquardt, and T. Asfour, "Ankle Exoskeleton with a Symmetric 3 DoF Structure for Plantarflexion Assistance," in *IEEE International Conference on Robotics and Automation (ICRA)*, Yokohama, Japan, 2024, (accepted).
- [6] H. S. Choi and Y. S. Baek, "Effects of the degree of freedom and assistance characteristics of powered ankle-foot orthoses on gait stability," *PLOS ONE*, vol. 15, no. 11, p. e0242000, Nov. 2020.
- [7] J. Olivier, A. Ortlieb, P. Bertusi, T. Vouga, M. Bouri, and H. Bleuler, "Impact of ankle locking on gait implications for the design of hip and knee exoskeletons," in *2015 IEEE International Conference on Rehabilitation Robotics (ICORR)*. IEEE, 2015, pp. 618–622.
- [8] E. M. McCain *et al.*, "Isolating the energetic and mechanical consequences of imposed reductions in ankle and knee flexion during gait," *Journal of NeuroEngineering and Rehabilitation*, vol. 18, no. 1, pp. 1–13, 2021.
- [9] R. Ranaweera *et al.*, "Effects of Restricting Ankle Joint Motions on Muscle Activity: Preliminary Investigation with an Unpowered Exoskeleton," in *2022 Moratuwa Engineering Research Conference (MERCCon)*. Moratuwa, Sri Lanka: IEEE, Jul. 2022, pp. 1–6.
- [10] J. H. Meuleman, E. H. Van Asseldonk, and H. Van der Kooij, "The effect of directional inertias added to pelvis and ankle on gait," *Journal of neuroengineering and rehabilitation*, vol. 10, no. 1, pp. 1–12, 2013.
- [11] R. C. Browning, J. R. Modica, R. Kram, and A. Goswami, "The effects of adding mass to the legs on the energetics and biomechanics of walking," *Medicine & Science in Sports & Exercise*, vol. 39, no. 3, pp. 515–525, 2007.
- [12] X. Jin, Y. Cai, A. Prado, and S. K. Agrawal, "Effects of exoskeleton weight and inertia on human walking," in *2017 IEEE International Conference on Robotics and Automation (ICRA)*. Singapore, Singapore: IEEE, May 2017, pp. 1772–1777.
- [13] L. Hak, H. Houdijk, P. J. Beek, and J. H. van Dieën, "Steps to take to enhance gait stability: the effect of stride frequency, stride length, and walking speed on local dynamic stability and margins of stability," *PloS one*, vol. 8, no. 12, p. e82842, 2013.
- [14] N. Aliman, R. Ramli, and S. M. Haris, "Design and development of lower limb exoskeletons: A survey," *Robotics and Autonomous Systems*, vol. 95, pp. 102–116, Sep. 2017.
- [15] D. Schmitthener, C. Sweeny, J. Du, and A. E. Martin, "The Effect of Stiff Foot Plate Length on Walking Gait Mechanics," *Journal of Biomechanical Engineering*, vol. 142, no. 9, p. 091012, Sep. 2020.